

RESEARCH ARTICLE



## Development of an apolipoprotein E mimetic peptide–lipid conjugate for efficient brain delivery of liposomes

Naoya Kato<sup>a</sup> , Sakura Yamada<sup>a,#</sup>, Rino Suzuki<sup>a</sup>, Yoshiki Iida<sup>a</sup>, Makoto Matsumoto<sup>a</sup>, Shintaro Fumoto<sup>a</sup> , Hidetoshi Arima<sup>b</sup>, Hidefumi Mukai<sup>a,c</sup> and Shigeru Kawakami<sup>a</sup> 

<sup>a</sup>Graduate School of Biomedical Sciences, Nagasaki University, Nagasaki, Japan; <sup>b</sup>School of Pharmacy, Daiichi University of Pharmacy, Fukuoka, Japan; <sup>c</sup>Laboratory for Molecular Delivery and Imaging Technology, RIKEN Center for Biosystems Dynamics Research, Hyogo, Japan

### ABSTRACT

Liposomes are versatile carriers that can encapsulate various drugs; however, for delivery to the brain, they must be modified with a targeting ligand or other modifications to provide blood–brain barrier (BBB) permeability, while avoiding rapid clearance by reticuloendothelial systems through polyethylene glycol (PEG) modification. BBB-penetrating peptides act as brain-targeting ligands. In this study, to achieve efficient brain delivery of liposomes, we screened the functionality of eight BBB-penetrating peptides reported previously, based on high-throughput quantitative evaluation methods with *in vitro* BBB permeability evaluation system using Transwell, *in situ* brain perfusion system, and others. For apolipoprotein E mimetic tandem dimer peptide (ApoEdp), which showed the best brain-targeting and BBB permeability in the comparative evaluation of eight peptides, its lipid conjugate with serine–glycine (SG)<sub>5</sub> spacer (ApoEdp-SG-lipid) was newly synthesized and ApoEdp-modified PEGylated liposomes were prepared. ApoEdp-modified PEGylated liposomes were effectively associated with human brain capillary endothelial cells via the ApoEdp sequence and permeated the membrane in an *in vitro* BBB model. Moreover, ApoEdp-modified PEGylated liposomes accumulated in the brain 3.9-fold higher than PEGylated liposomes in mice. In addition, the ability of ApoEdp-modified PEGylated liposomes to localize beyond the BBB into the brain parenchyma in mice was demonstrated via three-dimensional imaging with tissue clearing. These results suggest that ApoEdp-SG-lipid modification is an effective approach for endowing PEGylated liposomes with the brain-targeting ability and BBB permeability.

### ARTICLE HISTORY

Received 3 October 2022  
Revised 21 December 2022  
Accepted 26 December 2022

### KEYWORDS

Apolipoprotein E mimetic peptide; blood–brain barrier; brain-targeting; liposomes; tissue clearing

## 1. Introduction

With the increase in number of cases, the research and development of drugs for central nervous system (CNS) diseases has increased. However, drug delivery to the brain parenchyma via the systemic route is generally hampered by a very strong blood–brain barrier (BBB). Although the strength of the BBB varies with disease status, the delivery efficiency is remarkably low. Therefore, the development of brain-targeted drug delivery systems (DDSs) is essential to overcome the barrier (Ruan et al., 2021). Liposomes are versatile carriers that can encapsulate various drugs. Thus, brain-targeting of liposomes is expected to be an effective strategy. Surface modification of liposomes using polyethylene glycol (PEGylation) is useful for liposome delivery to the brain, avoiding rapid entrapment by reticuloendothelial systems (Nag & Awasthi, 2013). However, PEGylated liposomes cannot cross the BBB to brain parenchyma. Therefore, further modification of PEGylated liposomes with targeting ligands is a rational approach to overcome the BBB via adsorptive-mediated transcytosis (AMT) and receptor-mediated transcytosis (RMT) (Gao, 2016; Ogawa et al., 2020).

Over 1,200 types of BBB-penetrating peptides sequences have been reported by optimization of naturally occurring structures and exploration using phage display library screening (Kumar et al., 2021; Oller-Salvia et al., 2016). For DDS applications, peptide–drug conjugates have been preceded by clinical trials; for example, Angiopep-2 peptide–paclitaxel conjugate encoded as ANG1005 has been shown to reach targets in the CNS and meninges, and exhibited anti-tumor effects against leptomeningeal carcinomatosis and recurrent brain metastases in a phase 2 study (Kumthekar et al., 2020).

On the other hand, the development of BBB-penetrating peptide-modified liposomes remains a challenge. Glutathione-modified PEGylated liposomal doxorubicin encoded as 2B3-101 has been used in a phase 1/2a study in patients with solid tumors, brain metastases, or recurrent malignant glioma, but no significant difference in brain accumulation was observed compared with unmodified PEGylated liposomal doxorubicin in healthy mice (Gaillard et al., 2014). Rooy et al. compared five types of liposomes modified with brain-targeting ligands (holo-transferrin, RI7217, COG133, Angiopep-2, and CRM197); however, four types, except for RI7217, did not show efficient accumulation in the brain in

**CONTACT** Shigeru Kawakami  [skawakam@nagasaki-u.ac.jp](mailto:skawakam@nagasaki-u.ac.jp)  Graduate School of Biomedical Sciences, Nagasaki University, 1-7-1 Sakamoto, Nagasaki, 852-8588, Japan.

<sup>#</sup>Naoya Kato and Sakura Yamada are equally contributed

 Supplemental data for this article can be accessed online at <https://doi.org/10.1080/10717544.2023.2173333>.

© 2023 The Author(s). Published by Informa UK Limited, trading as Taylor & Francis Group.

This is an Open Access article distributed under the terms of the Creative Commons Attribution-NonCommercial License (<http://creativecommons.org/licenses/by-nc/4.0/>), which permits unrestricted non-commercial use, distribution, and reproduction in any medium, provided the original work is properly cited.

mice (van Rooy et al., 2011). They considered that the surface ligand density was fixed at one point and that there might be different optimal ligand densities corresponding to the target receptor. Therefore, it is difficult to compare the ligand functionality of nanoparticles. In addition, peptide ligand modifications of PEGylated liposomes must consider the possibility that the peptide ligand may be hidden in the PEG layer and fail to exhibit targeting abilities (Lehtinen et al., 2012). To overcome the PEG layer interference, we have demonstrated a proof-of-concept that ligand-SG-lipids, including a length-controlled serine-glycine ((SG)<sub>5</sub>) spacer to display the ligand outside the PEG layer (Hagimori et al., 2018; Kawakami & Suga, 2020; Suga et al., 2017, 2018). The ligand-SG-lipids have been provided targeting ability to PEGylated liposomes superior to that of commonly used ligand modification technology, ligand-PEG<sub>2000</sub>-lipid. This strategy may also be applied to the preparation of BBB-penetrating peptide-modified PEGylated liposomes but has not yet been validated.

In this study, we compared eight BBB-penetrating peptides reported previously in terms of different target receptors (Table 1). We found that the apolipoprotein E (ApoE) mimetic tandem dimer peptide (ApoEdp) has efficient brain-targeting ability via the permeability of the human brain capillary endothelial cell (hCMEC/D3) monolayers and brain accumulation in mice. In addition, we synthesized an ApoEdp-SG-lipid and prepared ApoEdp-modified PEGylated liposomes using the post-insertion method. We also evaluated the brain-targeting ability of ApoEdp-modified PEGylated liposomes, especially their BBB permeability using tissue clearing based intracerebral distribution analysis.

## 2. Materials and methods

### 2.1. Materials

Rink Amide AM resin was purchased from Merck KGaA (Darmstadt, Germany). Fluorescein isothiocyanate-dextran (mol wt 4,000 (FD-4) and mol wt 2,000,000 (FD-2000)) and 5(6)-carboxyfluorescein (CF) were purchased from Sigma-Aldrich Co. (St Louis, MO, USA). Palmitic acid was purchased from Nacalai Tesque, Inc. (Kyoto, Japan), while 1,2-distearoyl-*sn*-glycero-3-phosphocholine (DSPC) and 1,2-dioleoyl-*sn*-glycero-3-phosphoethanolamine-*N*-(lissamine rhodamine B sulfonyl) (ammonium salt) (rhodamine-DOPE) were purchased from Avanti Polar Lipids Inc. (Alabaster, AL, USA). *N*-(Carbonyl-methoxypolyethyleneglycol2000)-1,2-distearoyl-*sn*-glycero-3-phosphoethanolamine (mPEG<sub>2000</sub>-DSPE) was

purchased from the NOF Corporation (Tokyo, Japan). All other chemicals were reagent-grade commercially obtained products.

### 2.2. Synthesis of CF-labeled BBB-penetrating peptides and (dipalmitoyl)lysine-KSS-(SG)<sub>5</sub>-ApoEdp

CF-labeled BBB-penetrating peptides (Table 1) were synthesized based on the general solid-phase peptide synthesis procedure using Rink Amide AM resin. CF was coupled to the N-terminus of the peptide by the same coupling step. After completion of the reaction, each peptide was cleaved from the resin using trifluoroacetic acid (TFA)/triisopropylsilane (TIS)/distilled water (DW) (95/2.5/2.5, v/v/v) for 3 h. In the case of cysteine-containing sequence, TFA/TIS/DW/1,2-ethanedithiol (94/1/2.5/2.5, v/v/v/v) was used. The crude peptide was purified via reversed-phase high-performance liquid chromatography (RP-HPLC) and the mass of products was confirmed via matrix-assisted laser desorption-ionization time-of-flight mass spectrometry (MALDI-TOF-MS) (Figures S1–S16).

(Dipalmitoyl)lysine-KSS-(SG)<sub>5</sub>-ApoEdp (ApoEdp-SG-lipid) was synthesized based on the method described previously with peptide sequence changing (Suga et al., 2018). The crude lipid was purified via RP-HPLC and the mass of the products was confirmed via MALDI-TOF-MS (Figures S17, S18).

### 2.3. Preparation of liposomes

PEGylated liposomes were composed of DSPC and mPEG<sub>2000</sub>-DSPE (20:1 molar ratio). To label the PEGylated liposomes, rhodamine-DOPE (0.5 mol%), DiR (0.5 mol%), or Cy5.5-PEG<sub>2000</sub>-DSPE (0.5 mol%, a corresponding part of mPEG<sub>2000</sub>-DSPE was substituted) was incorporated. To prepare the ApoEdp-modified PEGylated liposomes, the lipid film hydration method and post-insertion method were performed as previously described (Kato et al., 2022). Physicochemical properties were measured using a Zetasizer Nano ZS system (Malvern Instruments Ltd., Worcestershire, UK).

### 2.4. Cell culture

Human brain capillary endothelial hCMEC/D3 cells were obtained from Merck (Darmstadt, Germany). hCMEC/D3 cells were seeded in the collagen-I coated flasks and cultured in EGM-2 Endothelial Cell Growth Medium-2 Bullet Kit (Lonza, Verviers, Belgium) containing growth factors and 5%

**Table 1.** Sequences and transport mechanisms of the BBB-penetrating peptides used in this study.

Name	Sequence	Target receptor	Reference
Angiopep-2	CF-GGG-TFFYGGSRGKRNNFKTEEY	LRP1 (RMT)	(Demeule et al., 2008)
ApoEdp	CF-GGG-LRKLRKRLLRKLRKRL	LDLR, LRP1, LRP2 (RMT)	(Wang et al., 2013)
CDX	CF-GGG-FKESWREARGTRIERG	nAChR (RMT)	(Zhan et al., 2011)
HAI	CF-GGG-HAIYPRH	TfR (RMT)	(Lee et al., 2001)
SynB1	CF-GGG-RGGRLSYRRRFSTSTGR	AMT	(Rousselle et al., 2000)
Tat	CF-GGG-YGRKKRRQRRR	AMT	(Schwarze et al., 1999)
LNP	CF-GGG-KKRTLKNDKRC	AMT	(Yao et al., 2015)
#2077	CF-GGG-RLSSVDSLSGC	Unknown	(Urich et al., 2015)

Abbreviations: CF, carboxyfluorescein; LRP1, low-density lipoprotein receptor-related protein 1; RMT, receptor-mediated transcytosis; LDLR, low-density lipoprotein receptor; LRP2, low-density lipoprotein receptor-related protein 2; nAChR, nicotinic acetylcholine receptor; TfR, transferrin receptor; AMT, adsorptive-mediated transcytosis.

heat-inactivated fetal bovine serum (AusGene X, Brisbane, Australia) at 37°C in 5% CO<sub>2</sub>.

## 2.5. Cellular association experiments

hCMEC/D3 cells were seeded in 5 µg/cm<sup>2</sup> rat tail collagen I (Thermo Fisher Scientific Inc., MA, USA)-precoated 24 well plates (5 × 10<sup>4</sup> cells/cm<sup>2</sup>). To evaluate the BBB-penetrating peptides, after 24 h of incubation, the cells were incubated with CF-labeled peptides (10 µM) in EGM-2 medium for 1 h. To evaluate the liposomes, the cells were incubated with rhodamine-labeled liposomes for 3 h. For competitive inhibition studies, the cells were co-incubated with each liposome in the presence of poly-L-lysine (10 µM) or heparin (10 unit/mL) for 1 h. The cells were collected and washed with 1 × phosphate buffered saline (PBS (-), pH 7.4). After washing, the cell pellets were dispersed in 1 × PBS (-) and evaluated using flow cytometry (BD LSR Fortessa X-20 Cell Analyzer; BD Biosciences, San Jose, CA, USA).

## 2.6. In vitro BBB permeability assay

hCMEC/D3 cells were seeded at a density of 2 × 10<sup>5</sup> cells/cm<sup>2</sup> in rat tail collagen I-precoated (5 µg/cm<sup>2</sup>) 12-well Transwell plates (Corning, New York, USA) and cultured for seven days by changing the medium every 2–3 d. Transepithelial electrical resistance (TEER) was measured for tight junction integrity using Millicell ERS-2 (Merck Millipore, Bedford, MA, USA). TEER of hCMEC/D3 cell monolayers [Ω.cm<sup>2</sup>] were calculated using the following equations:

$$\text{TEER}[\Omega \cdot \text{cm}^2] = (R_{\text{monolayer}} - R_{\text{blank}}) \times A$$

where  $R_{\text{monolayer}}$  is the resistance across the cell monolayers on the insert membrane,  $R_{\text{blank}}$  is the resistance of the membrane only, and  $A$  is the membrane surface area (1.12 cm<sup>2</sup>). In accordance with previous reports that strong hCMEC/D3 cell monolayers are formed when this value is 20 Ω.cm<sup>2</sup> or higher, the wells with cell monolayers that fulfilled this condition were used for the experiments (Eigenmann et al., 2013; Weksler et al., 2013). To evaluate the BBB-penetrating peptides, the medium on the apical side was replaced with CF-labeled peptides (10 µM) in EGM-2 and incubated for 3 h. To evaluate the liposomes, the medium on the apical side was replaced with rhodamine-labeled liposomes (100 µM) in EGM-2 and incubated for 24 h. After incubation for appropriate hours, the solution was collected from the basal side and fluorescence was measured using a Gemini XPS microplate reader (Molecular Devices, Sunnyvale, CA, USA). The transport ratio (T [%]) and apparent permeability coefficient (Papp) [cm/s] were calculated using the following equations:

$$T[\%] = \left( \frac{\Delta[C]_{\text{basal}}}{[C_0]_{\text{apical}}} \right) \times 100$$

$$\text{Papp}[\text{cm}/\text{s}] = \left\{ V_{\text{basal}} / \left( A \times [C_0]_{\text{apical}} \right) \right\} \times \left( \Delta[C]_{\text{basal}} / \Delta t \right)$$

where  $V_{\text{basal}}$  is the volume of the medium on the basal side (1 cm<sup>3</sup>),  $A$  is the membrane surface area (1.12 cm<sup>2</sup>), and  $\Delta t$  is the time of the experiment.  $[C_0]_{\text{apical}}$  is the initial fluorescent concentration and  $\Delta[C]_{\text{basal}}$  is the detected value of the fluorescent concentration on the basal side at an appropriate time.

## 2.7. Animal

Five-week-old male ddY mice were purchased from Japan SLC, Inc. (Shizuoka, Japan). The mice were housed in an air-conditioned room with free access to water and a standard laboratory diet (CE-2, CLEA Japan, Inc., Tokyo, Japan).

## 2.8. In situ transcardiac brain perfusion

CF-labeled peptides (5 µM) were transcardially perfused at a rate of 2 mL/min for 2 min, as described previously (Matsui et al., 2020). To eliminate the CF-containing perfusate, further perfusion using PBS (-) solution was performed for 10 min. Then, the brain was collected, homogenized with 500 µL of 0.5 M borate buffer (pH 10.0), and centrifuged (1,000 g, 4°C, 15 min). The brain homogenate was mixed with 500 µL of 99.5% ethanol and centrifuged (15,000 g, 4°C, 15 min). Fluorescence of the supernatant was measured using a SpectraMax iD3 microplate reader (Molecular Devices, Sunnyvale, CA, USA). Brain/Perfusate ratio [µL/g] was calculated using the following equations:

$$\text{Brain/Perfusate ratio} [\mu\text{L}/\text{g}] = (\text{fluorescence}/\text{g of brain}) / (\text{fluorescence}/\mu\text{L of perfusate})$$

## 2.9. Brain accumulation after intravenous injection

For the evaluation of BBB-penetrating peptides, mice were intravenously injected with CF-labeled peptides (1.67 µmol fluorescein/kg). One hour after injection, the brain was collected and homogenized. For the evaluation of liposomes, DiR-labeled liposomes (0.25 µmol DiR/kg) were intravenously injected in mice. Twenty-four hours after injection, the brain was collected and homogenized. The obtained brain homogenate was centrifuged (15,000 g, 4°C, 5 min). The fluorescence of the supernatant was measured using a Gemini XPS microplate reader. The percent injected dose per g brain [%ID/g brain] was calculated by substituting the sample fluorescence into the calibration curves using prepared supernatant from the injected sample and a non-treated fresh brain.

## 2.10. Intracerebral distribution using three-dimensional imaging

After the intravenous injection of CF-labeled peptides (1.67 µmol fluorescein/kg) or Cy5.5-labeled liposomes (0.25 µmol Cy5.5/kg), the mice were perfused with heparinized PBS (-) (10 units/mL), followed by PBS (-) through the left ventricle. Vessel staining was performed by perfusion of 10 mL Dil solution (120 µM). Then perfusion and fixation with 4% paraformaldehyde (PFA) were performed as described previously (Li et al., 2008). The brain

was collected and further immersed in 4% PFA overnight. The fixed brain was then immersed in Seebest-PP (pH 7.4) for 24h according to the previous report (Fumoto et al., 2020). Confocal images were acquired using a LSM710 confocal microscope (Carl Zeiss, Oberkochen, Germany).

### 2.11. Statistical analysis

Statistical analysis of the data was performed using a two-tailed unpaired *t*-test, one-way analysis of variance (ANOVA) followed by Dunnett's test or Tukey's test, and two-way repeated-measures ANOVA followed by Tukey's test. Data are represented as the mean  $\pm$  standard deviation (S.D.).

## 3. Results

### 3.1. Cellular association and monolayer permeability of BBB-penetrating peptides

As control groups, CF, the compound used for the fluorescent labeling of peptides, and FD-4, a fluorescein-labeled compound with a molecular weight comparable to that of the peptides, were selected. In the cellular association experiment, Tat, ApoEdp, and LNP peptides were one order of magnitude higher than those in the other groups (Figure 1). In the hCMEC/D3 cell monolayer permeability test, six BBB-penetrating peptides, except for #2077 and LNP peptides, showed significantly higher permeability than FD-4 (Figure 2 and Table S1). Therefore, six BBB-penetrating peptides (Angiopep-2, ApoEdp, CDX, HAI, SynB1, and Tat) were used for further experiments.

### 3.2. Intracerebral accumulation and localization of BBB-penetrating peptides

To validate BBB permeability in mice, we selected two types of evaluation methods: *in situ* transcardiac brain perfusion and intravenous injection. *In situ* transcardiac brain perfusion allows easy assessment of BBB permeability of intact peptides. In contrast, the intravenous injection approach is the most common, and it affects blood stability and accumulation

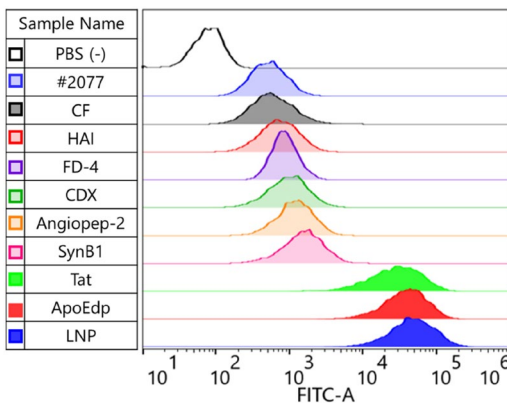


**Figure 1.** Cellular association experiments of CF-labeled BBB-penetrating peptides in hCMEC/D3 cells. The cells were incubated with each compound at 37°C for 1h.

in other organs. In both experiments, the brain accumulation of all BBB-penetrating peptides showed much higher values than FD-4, especially ApoEdp (Figure 3). To confirm the effective brain accumulation of ApoEdp beyond the BBB, three-dimensional imaging was performed using a tissue-clearing reagent. Seebest-PP was selected as the tissue clearing reagent because of its high lipophilic dye retention

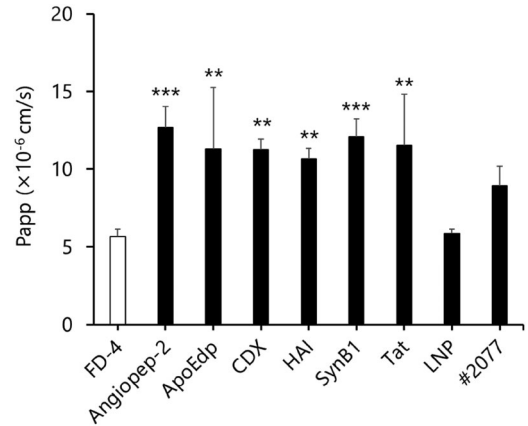


**Figure 2.** Transcytosis efficiency of CF-labeled BBB-penetrating peptides across hCMEC/D3 cell monolayers. Each compound was added to the apical side and the fluorescence was measured in the basal side after 3h. Data are represented as the mean  $\pm$  S.D. of quadruplicate. Significant differences are represented as \*\**P* < 0.01, \*\*\**P* < 0.001 (Dunnett's test).

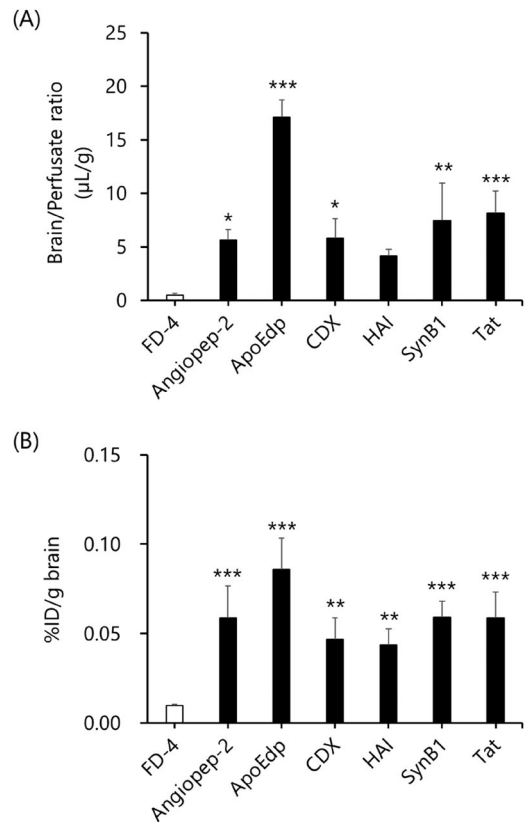


**Figure 3.** Brain accumulation of CF-labeled BBB-penetrating peptides in mice. (A) *In situ* transcardiac brain perfusion of each compound at the rate of 2 mL/min for 2 min. (B) Intravenous injection of each compound at 1 h post-injection. Data are represented as the mean  $\pm$  S.D. ((A) *n* = 3, (B) *n* = 4). Significant differences are represented as \**P* < 0.05, \*\**P* < 0.01, \*\*\**P* < 0.001 (Dunnett's test).

and deep observation capability (Figure S19). BBB-impermeable FD-2000 was used as the control group (Uwamori et al., 2019). The confocal image of FD-2000 did not show green fluorescence signals derived from fluorescein, indicating the integrity of the BBB (Figure 4A and D). Meanwhile, the images of ApoEdp in different regions clearly showed green fluorescence signals at the point indicated by white arrows that did not merge with the Dil-derived red signals (Figure 4B, C, E, and F). Based on comparative studies of eight BBB-penetrating peptides, ApoEdp was selected as the BBB-penetrating peptide for further experiments.

### 3.3. Preparation and characterization of liposomes

To prepare the brain-targeted PEGylated liposomes, ApoEdp-SG-lipid was synthesized via solid-phase peptide synthesis, and a purity of over 95% was used (Figures 5A, S17, and S18). ApoEdp-modified PEGylated liposomes were prepared by mixing PEGylated liposomes with 0.25, 0.5, or 1.0 mol% ApoEdp-SG-lipid to the total lipid mol (Figure 5B). The size of each liposome was approximately 80 nm, and the polydispersity index (PDI) showed monodispersibility at approximately 0.2. The zeta potential slightly increased according to the ApoEdp-SG-lipid modification (Table 2).

### 3.4. BBB targeting study of ApoEdp-modified PEGylated liposomes *in vitro*

To evaluate the functionality of ApoEdp-modified PEGylated liposomes, we examined the cellular association and monolayer

permeability of hCMEC/D3 cells. The cellular association of ApoEdp-modified PEGylated liposomes with any modification amount was much higher than that of PEGylated liposomes, and the mean fluorescence intensity significantly increased as the modification amount increased (Figure 6). At each liposome concentration (25, 50, and 100  $\mu\text{M}$ ) and incubation time (1, 2, and 3 h), the cellular association of 1.0 mol% ApoEdp-modified PEGylated liposomes was also much higher than that of PEGylated liposomes (Figure S20). To confirm the association of ApoEdp-modified PEGylated liposomes to hCMEC/D3 cells via ApoEdp, competitive inhibition experiments were performed. Heparin is a competitive compound with a 142–147 sequence (RKLRRK) of ApoE (Libeu et al., 2001). Poly-L-lysine is an inhibitor of heparan sulfate proteoglycan (HSPG) that partly mediates ApoE binding to the low-density lipoprotein receptor (LDLR) family (Sauer et al., 2005). The cellular association of ApoEdp-modified PEGylated liposomes drastically decreased in the presence of these inhibitors. In particular, cellular association of ApoEdp-modified PEGylated liposomes treated with heparin were decreased to the same extent as the PEGylated liposomes (Figure 7). Monolayer permeability was evaluated using an *in vitro* BBB model to examine the transcytosis efficiency of the ApoEdp-modified PEGylated liposomes. ApoEdp-modified PEGylated liposomes exhibited a higher T [%] over time (Table S2). Papp value of 0.25, 0.5, or 1.0 mol% ApoEdp-modified PEGylated liposome was significantly increased compared to that of PEGylated liposomes from  $2.61 \times 10^{-7}$  to  $1.14 \times 10^{-6}$ ,  $1.26 \times 10^{-6}$ , and  $1.32 \times 10^{-6}$  [cm/s] (Figure 8). Therefore, 1.0 mol% ApoEdp-modified liposomes were used *in vivo* further experiments because they showed the highest values in both Figures 6 and 8.

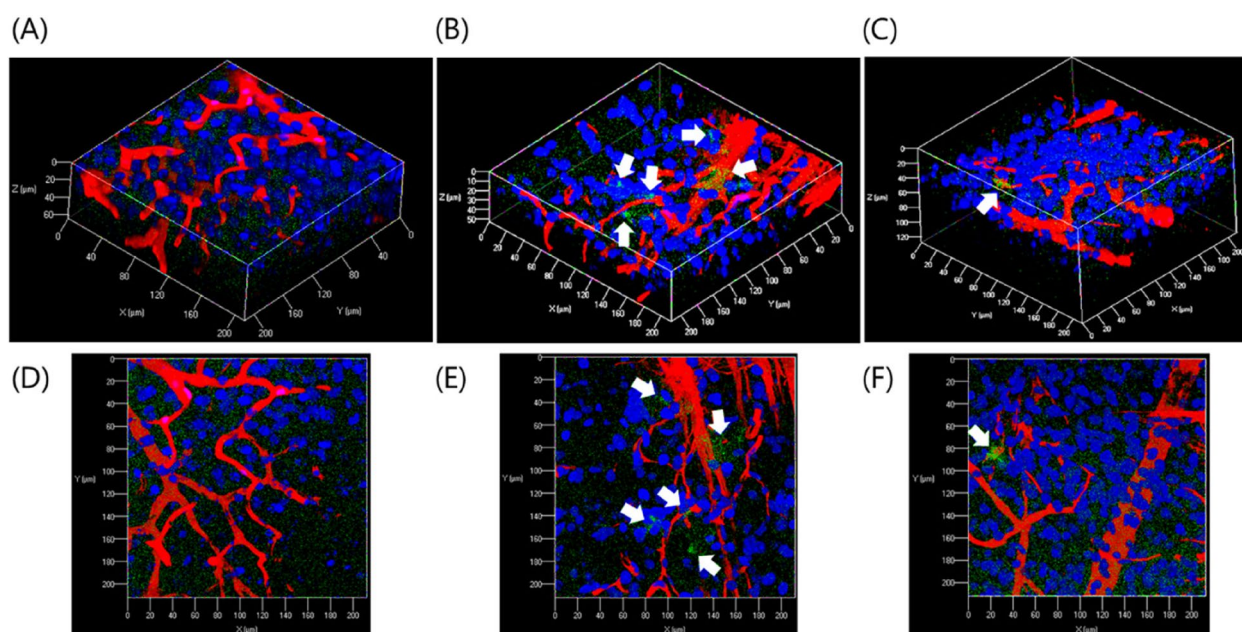


**Figure 4.** Intracerebral distribution analysis using three-dimensional imaging. One hour after intravenous injection, cerebral blood vessels were stained, and the brain was fixed and immersed in Seebest-PP (pH 7.4) for 24 h. Confocal microscopy images of the intracerebral distribution of (A) BBB-impermeable FD-2000, (B) and (C) CF-labeled ApoEdp at different regions. (D-F) show the top view of (A-C), respectively. Nuclei and cerebral blood vessels were stained with 4, 6-diamino-2-phenylindole (DAPI) (blue) and Dil (red), respectively. Each compound was detected by the fluorescence of fluorescein or CF (green). White arrows indicate ApoEdp localization outside of cerebral blood vessels.

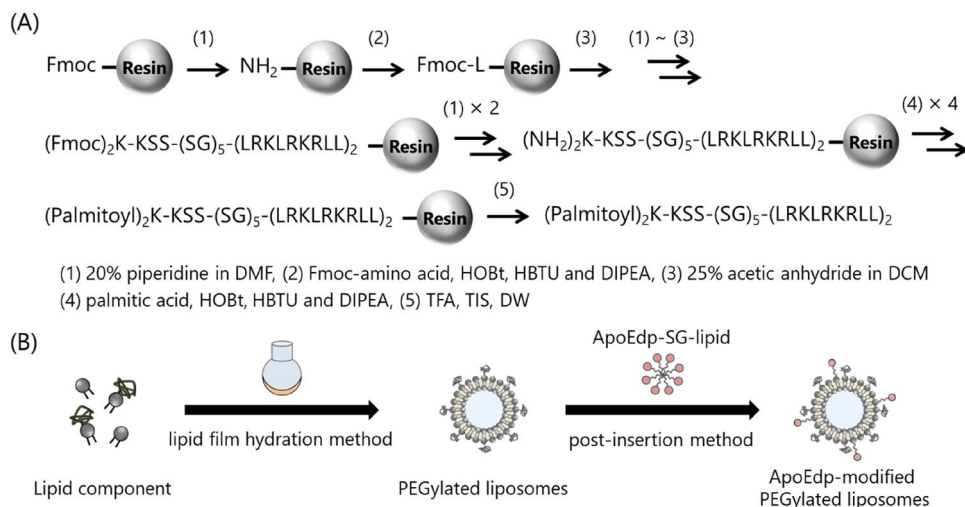


**Figure 5.** Schematic diagrams of (A) synthesis of ApoEdp-SG-lipid using solid-phase peptide synthesis and (B) preparation of ApoEdp-modified PEGylated liposomes. Abbreviations: Fmoc, 9-fluorenylmethyloxycarbonyl; DMF, *N,N*-dimethylformamide; HOBt, 1-hydroxybenzotriazole; HBTU, 1-[bis(dimethylamino)methylene]-1*H*-benzotriazolium 3-oxide hexafluorophosphate; DIPEA, *N,N*-diisopropylethylamine; DCM, dichloromethane; TFA, trifluoroacetic acid; TIS, triisopropylsilane; DW, distilled water.

### 3.5. Intracerebral accumulation and distribution of ApoEdp-modified PEGylated liposomes *in vivo*

Brain-targeted nanoparticles tend to accumulate in the healthy brain via transcytosis at 24 h intravenous post-injection (Bana et al., 2014; Huwyler et al., 1996; Kucharz et al., 2021). Therefore, twenty-four hours after intravenous injection in mice, brain accumulation was evaluated to determine the functionality of the ApoEdp-modified PEGylated liposomes. The brain uptake [%ID/g brain] of 1.0 mol% ApoEdp-modified PEGylated liposomes was significantly higher (3.9-fold) than that of PEGylated liposomes. The value of ApoEdp-modified PEGylated liposomes was 0.85 [%ID/g brain], while that of PEGylated liposomes was 0.22 [%ID/g brain] (Figure 9). To clarify the entry of 1.0 mol% ApoEdp-modified PEGylated liposomes into the brain parenchyma, three-dimensional imaging using Seebest-PP was performed. In the case of PEGylated liposomes, only white signals (the result of merging red and cyan signals) were detected, indicating the liposomes were located in the cerebral blood vessels (Figure 10A, C and D). In contrast, the images of 1.0 mol% ApoEdp-modified PEGylated liposomes were observed not only as white signals but also as cyan signals, indicating the liposomes were partly distributed outside the cerebral blood vessels (Figure 10B, E and F).

## 4. Discussion

In this study, ApoEdp was determined as the best brain-targeting and BBB-penetrating peptide in the comparative evaluation of eight peptides. ApoEdp is a tandem dimeric peptide derived

from ApoE and has been reported to have better brain-targeting ability than the monomer in various experiments (Morito et al., 2021; Re et al., 2011). Its lipid conjugate with (SG)<sub>5</sub> linker was newly synthesized, and ApoEdp-modified PEGylated liposomes were prepared. In addition, the ability of ApoEdp-modified PEGylated liposomes to localize into the brain parenchyma beyond the BBB in mice was demonstrated via three-dimensional imaging with tissue clearing.

We have screened eight BBB-penetrating peptides based on the combined evaluation. This combination enabled us to evaluate robust brain-targeting ability. In flow cytometry, Tat, ApoEdp, and LNP peptides showed high affinity for hCMEC/D3 cells more than one order of magnitude higher than the other peptides. However, *in vitro* BBB permeabilities of six peptides were high and comparable except for those of #2077 and LNP peptides (Figures 1–2, Table S1). BBB permeation mechanisms of the peptides evaluated in this study were diverse, including RMT and AMT, and no correlation was observed between such mechanistic differences and *in vitro* BBB cellular association/permeation efficiency (Table 1). In particular, low *in vitro* BBB permeability of LNP peptide showed seemingly inconsistent with the high cellular association. In the transcytosis process of peptides/antibodies, binding affinity to target receptors or cellular membranes is an important factor (Bach et al., 2012; Couch et al., 2013; Kristensen et al., 2020; Niewoehner et al., 2014). That is, if the association is too slow, the peptides/antibodies cannot be taken up by cerebral vascular endothelial cells, while if the dissociation is too slow after association, they are retained in the endosomes and cannot penetrate the BBB. Therefore, the LNP peptide is considered unsuitable as a

**Table 2.** Physicochemical properties of liposomes ( $n=3$ ).

	Size (d.nm)	PDI	ζ-potential (mV)
PEGylated liposomes	85.0 ± 15.7	0.26 ± 0.05	-1.08 ± 1.20
0.25 mol% ApoEdp-modified PEGylated liposomes	76.1 ± 2.9	0.15 ± 0.05	-0.16 ± 1.35
0.5 mol% ApoEdp-modified PEGylated liposomes	84.5 ± 6.6	0.14 ± 0.04	0.39 ± 1.32
1.0 mol% ApoEdp-modified PEGylated liposomes	82.8 ± 4.2	0.18 ± 0.04	0.82 ± 1.08

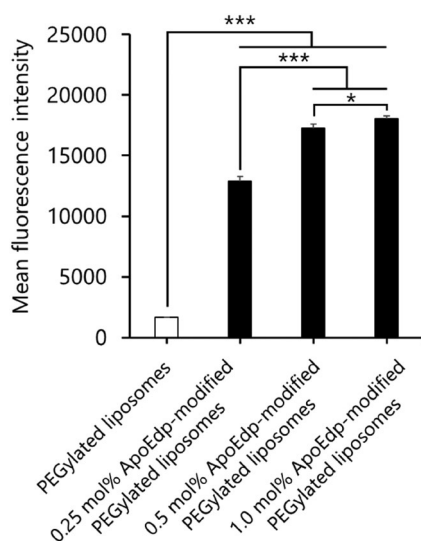


**Figure 6.** Cellular association experiments of rhodamine-labeled liposomes in hCMEC/D3 cells. The cells were incubated with each liposome for 3 h at a concentration of 100  $\mu$ M. Data are the mean  $\pm$  S.D. for triplicate experiments. \* $P < 0.05$ , \*\*\* $P < 0.001$  (Tukey's test).

brain-targeting ligand for modifying PEGylated liposomes because of its inefficient dissociation from the membranes of cerebral endothelial cells. Similarly, for the BBB permeability of Tat and ApoEdp, most of the effects of high cellular association were likely offset by their low dissociation.

In the *in vivo* evaluation of the brain-targeting efficiency under various conditions, including the influence of the presence of blood components, the trends in efficiency obtained with *in situ* brain perfusion and systemic administration systems were similar, with ApoEdp being the most efficient (Figure 3). Regarding the sensitivity of detecting differences in the brain-targeting ability of peptides, the *in situ* perfusion system is better, as the effect of systemic biodistribution is ignored. Because of the slow clearance of PEGylated liposomes, it is appropriate to discuss the result in a perfusion system, which can be assessed the first-pass effect of peptides on the brain. The high brain-targeting efficiency of ApoEdp may be due to its ability to target multiple receptors, including LDLR, low-density lipoprotein receptor-related protein (LRP)-1, and LRP-2. Most importantly, Histological studies demonstrated that ApoEdp can leak from the cerebral blood vessels and distribute in the brain parenchyma (Figure 4); therefore, we selected ApoEdp as the peptide for PEGylated liposome modification.

ApoEdp-SG-lipid was successfully synthesized with high purity using the solid-phase peptide synthesis method and showed a single molecular weight distribution pattern (Figures 5A, S17, and S18). This is in contrast to the very low reaction efficiency of ApoEdp-PEG-lipid synthesized by thiol-maleimide coupling using a conventional PEG spacer (Figure S21). Because ApoEdp-SG-lipid has excellent aqueous dispersibility, it was possible to modify PEGylated liposomes using the post-insertion approach (Figure 5B). Modification of ApoEdp-SG-lipid by only 0.25 mol% markedly improved the association of PEGylated liposomes with hCMEC/D3 cells and their *in vitro* BBB permeability, and the efficiency tended to

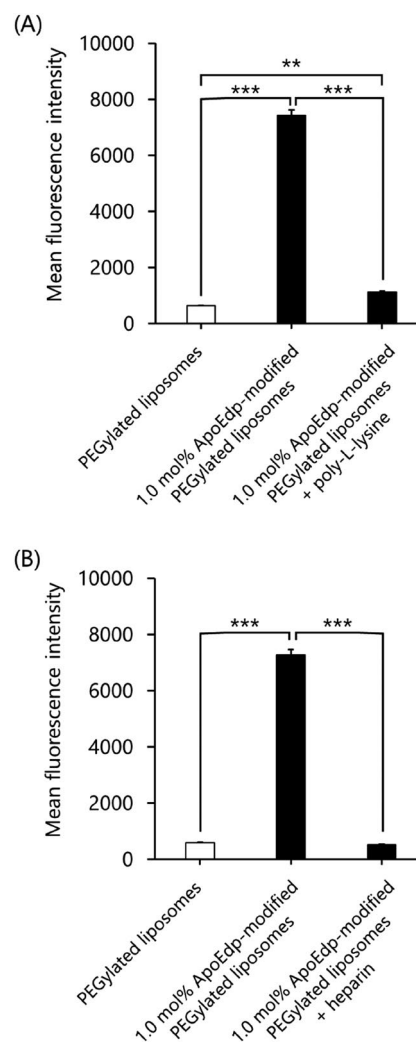


**Figure 7.** Competitive inhibition experiments of rhodamine-labeled liposomes in hCMEC/D3 cells. The cells were co-incubated with the liposome in the presence of (A) poly-L-lysine or (B) heparin for 1 h. Data are the mean  $\pm$  S.D. for triplicate experiments. \*\* $P < 0.01$ , \*\*\* $P < 0.001$  (Tukey's test).

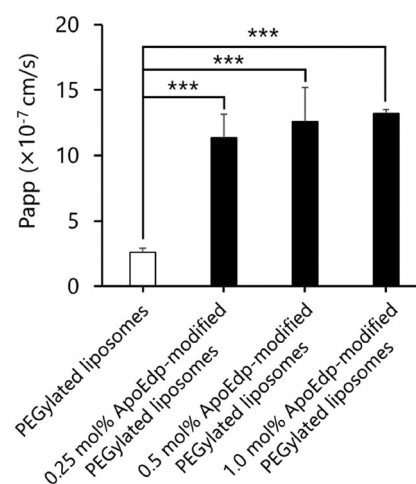


**Figure 8.** Transcytosis efficiency of rhodamine-labeled liposomes across hCMEC/D3 cell monolayers. Each liposome was added to the apical side and the fluorescence was measured in the basal side after 24 h. Data are represented as the mean  $\pm$  S.D. of quadruplicate. Significant differences are represented as \*\*\* $P < 0.001$  (Tukey's test).

saturate when the modification amount was increased to 1.0 mol% (Figures 6 and 8). Importantly, the post-insertion of ApoE<sub>p</sub>-SG-lipid did not change the particle size of the liposomes, and their PDI values remained monodisperse around 0.2 (Table 2). A slight increase in zeta potential may indicate the successful modification of the liposomes with ApoE<sub>p</sub>-SG-lipid. Treatment with poly-L-lysine and heparin markedly reduced the association with hCMEC/D3 cells of ApoE<sub>p</sub>-modified PEGylated liposomes (Figure 7), suggesting some of the brain-targeting ability and BBB permeability of ApoE<sub>p</sub>-modified PEGylated liposomes were probably mediated by the interaction of ApoE<sub>p</sub> with HSPG (Sauer et al., 2005). The tissue distribution experiments in mice showed that 1.0 mol% ApoE<sub>p</sub> modification resulted in 0.85 [%ID/g

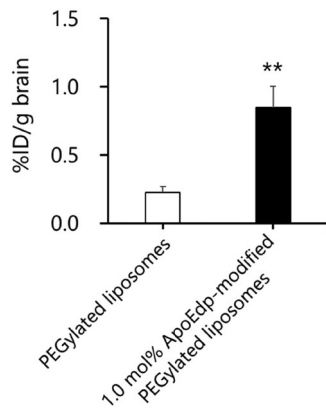


**Figure 9.** Brain accumulation of DiR-labeled liposomes in mice. Each liposome was injected intravenously, and the brain was collected after 24 h. Data are represented as the mean ± S.D. ( $n=3$ ). Significant differences are represented as  $**P < 0.01$  (two-tailed unpaired  $t$ -test).

brain], 3.9-fold higher than that of PEGylated liposomes (Figure 9). This result is superior to the glutathione-modified PEGylated liposomes (1.5-fold) (Gaillard et al., 2014). Histological studies demonstrated that PEGylated liposomes remained in the cerebral blood vessels. In contrast, 1.0 mol% ApoE<sub>p</sub>-modified PEGylated liposomes were distributed both inside and outside the cerebral blood vessels (Figure 10). The cyan signals seen in Figure 10B and F the accumulation at relatively easy to transcytosed areas such as post-capillary venules (Kucharz et al., 2021). These results suggest that ApoE<sub>p</sub>-SG-lipid modification of PEGylated liposomes can improve their brain-targeting ability and partly pass through the BBB into the brain.

In histological studies, three-dimensional imaging was performed using a tissue-clearing reagent. To evaluate the intratissue distribution of liposome formulations, surfactant-free tissue clearing reagents were used to prevent fluorescent-labeled liposomes and lipophilic fluorescent dyes for staining blood vessels from leaking out during the tissue clearing process (Figure S19). We have demonstrated the distribution of gene expression in the brain and the localization of PEGylated liposomes in colorectal cancer via three-dimensional imaging using Scale SQ(0), a surfactant-free tissue-clearing reagent (Ogawa et al., 2018; Suga et al., 2018). Furthermore, we developed a new surfactant-free tissue-clearing reagent, Seebest-PP, and demonstrated its superiority as a DDS evaluation method (Fumoto et al., 2020). The histological results of this study strongly show that three-dimensional imaging using Seebest-PP can be useful for evaluating the distribution of liposomes and other DDS formulations in the brain, especially the relationship between their localization in cerebral blood vessels. We

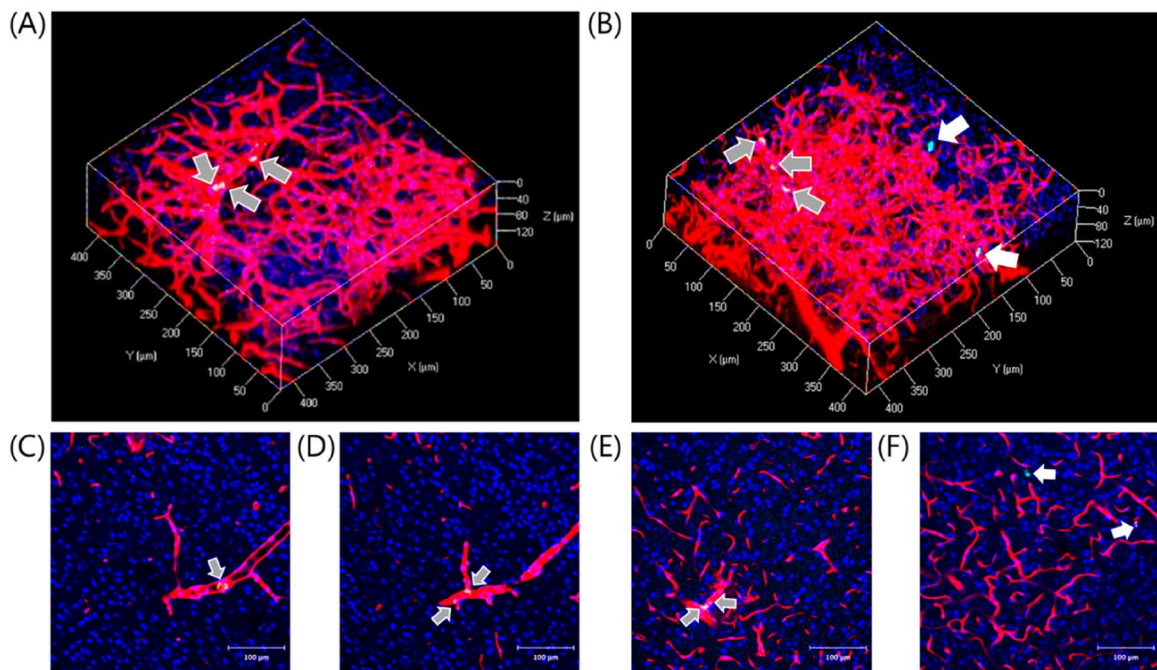


**Figure 10.** Intracerebral distribution of Cy5.5-labeled liposomes using three-dimensional imaging. Twenty-four hours after intravenous injection, cerebral blood vessels were stained, and the brain was fixed and immersed in Seebest-PP (pH 7.4) for 24 h. (A) and (B) show the spatial distribution of Cy5.5-labeled PEGylated liposomes and 1.0 mol% ApoE<sub>p</sub>-modified PEGylated liposomes, respectively. (C), (D) and (E), (F) show the two-dimensional images of (A) and (B). Nuclei and cerebral blood vessels were stained with DAPI (blue) and Dil (red), respectively. Each liposome was detected by the fluorescence of Cy5.5 (cyan). Gray and white arrows indicate the localization inside and outside the blood vessels, respectively.

believe that this information will be valuable for the evaluation of the targeted delivery of liposomes to the brain.

Among the drugs used for CNS diseases, glioma requires a new DDS formulation. ApoEdp is a targeting ligand of gliomas as well as the BBB; therefore, ApoEdp-modified PEGylated liposomes are also expected to be delivery carriers of anticancer drugs, such as temozolomide, for glioma beyond the BBB (Yasaswi et al., 2021). ApoE mimetic peptide-grafted gold liposomes and polymersomes can reach gliomas beyond the BBB and exhibit anti-tumor effects (Grafals-Ruiz et al., 2020; Jiang et al., 2018). These formulations were prepared using bottom-up approaches by incorporating ApoE mimetic peptide-polymer conjugates into the component or designing to have reactive groups on the particle surface for post-conjugating the ligand. In contrast, the ApoEdp-SG-lipid developed in this study might be applicable to be easily modified in one-step by mixing with pre-formed drug-encapsulated PEGylated liposomes, which will be beneficial for practical applications (Kato et al., 2022).

## 5. Conclusion

In this study, we found ApoEdp, which accumulates in the brain more efficiently than other peptides, through a comprehensive analysis of eight potent BBB-penetrating peptides reported previously. We synthesized ApoEdp-SG-lipid with a single molecular weight distribution and found that ApoEdp-modified PEGylated liposomes could be prepared without affecting the size of the PEGylated liposomes by mixing with ApoEdp-SG-lipid. We also found that ApoEdp-SG-lipid modification for PEGylated liposomes could result in higher brain accumulation and partial localization in the brain beyond cerebral blood vessels using tissue clearing. These findings are valuable for the development and analysis of brain-targeted DDSs using liposomes.

## Acknowledgments

This study was partially supported by Nagai Memorial Research Scholarship from the Pharmaceutical Society of Japan (NK). This study used research equipment shared by the MEXT Project to promote the public utilization of advanced research infrastructure (Program for supporting the introduction of the new sharing system; grant number JPMXS0422500320).

## Disclosure statement

The author reports no conflicts of interest in this work.

## Ethical Approval statement

All animal experiments were performed in accordance with the Guide for Animal Experimentation of Nagasaki University (Approval number, 1812251497-7).

## Funding

This study was partially supported by JSPS KAKENHI grant number 20H04540 (HA), Grant-in-Aid for JSPS Fellows JP20J21334 (NK), and

Center for Clinical and Translational Research of Kyushu University Hospital (SK).

## ORCID

Naoya Kato  <http://orcid.org/0000-0001-8233-5426>

Shintaro Fumoto  <http://orcid.org/0000-0002-2218-4547>

Shigeru Kawakami  <http://orcid.org/0000-0001-8765-2463>

## References

- Bach A, Clausen BH, Møller M, et al. (2012). A high-affinity, dimeric inhibitor of PSD-95 bivalently interacts with PDZ1-2 and protects against ischemic brain damage. *Proc Natl Acad Sci U S A* 109:1–10.
- Bana L, Minniti S, Salvati E, et al. (2014). Liposomes bi-functionalized with phosphatidic acid and an ApoE-derived peptide affect A $\beta$  aggregation features and cross the blood-brain-barrier: implications for therapy of Alzheimer disease. *Nanomedicine* 10:1583–90.
- Couch JA, Yu YJ, Zhang Y, et al. (2013). Addressing safety liabilities of TFR bispecific antibodies that cross the blood-brain barrier. *Sci Transl Med* 5:183ra57.
- Demeule M, Régina A, Ché C, et al. (2008). Identification and design of peptides as a new drug delivery system for the brain. *J Pharmacol Exp Ther* 324:1064–72.
- Eigenmann DE, Xue G, Kim KS, et al. (2013). Comparative study of four immortalized human brain capillary endothelial cell lines, hCMEC/D3, hBMEC, TY10, and BB19, and optimization of culture conditions, for an in vitro blood-brain barrier model for drug permeability studies. *Fluids Barriers CNS* 10:33.
- Fumoto S, Kinoshita E, Ohta K, et al. (2020). A pH-adjustable tissue clearing solution that preserves lipid ultrastructures: suitable tissue clearing method for DDS evaluation. *Pharmaceutics* 12:1070.
- Gaillard PJ, Appeldoorn CCM, Dorland R, et al. (2014). Pharmacokinetics, brain delivery, and efficacy in brain tumor-bearing mice of glutathione pegylated liposomal doxorubicin (2B3-101). *PLoS One* 9:e82331.
- Gao H. (2016). Progress and perspectives on targeting nanoparticles for brain drug delivery. *Acta Pharm Sin B* 6:268–86.
- Grafals-Ruiz N, Rios-Vicil CI, Lozada-Delgado EL, et al. (2020). Brain targeted gold liposomes improve rna1 delivery for glioblastoma. *Int J Nanomedicine* 15:2809–28.
- Hagimori M, Chinda Y, Suga T, et al. (2018). Synthesis of high functionality and quality mannose-grafted lipids to produce macrophage-targeted liposomes. *Eur J Pharm Sci* 123:153–61.
- Huwylar J, Wu D, Pardridge WM. (1996). Brain drug delivery of small molecules using immunoliposomes. *Proc Natl Acad Sci U S A* 93:14164–9.
- Jiang Y, Zhang J, Meng F, Zhong Z. (2018). Apolipoprotein E peptide-directed chimeric polymersomes mediate an ultrahigh-efficiency targeted protein therapy for glioblastoma. *ACS Nano* 12:11070–9.
- Kato N, Sato T, Fuchigami Y, et al. (2022). Synthesis and evaluation of a novel adapter lipid derivative for preparation of cyclic peptide-modified PEGylated liposomes: application of cyclic RGD peptide. *Eur J Pharm Sci* 176:106239.
- Kawakami S, Suga T. (2020). Development of Nano-DDS carriers for control of spatial distribution using multi-color deep imaging. *Yakugaku Zasshi* 140:633–40.
- Kristensen M, Kucharz K, Felipe Alves Fernandes E, et al. (2020). Conjugation of therapeutic PSD-95 inhibitors to the cell-penetrating peptide tat affects blood-brain barrier adherence, uptake, and permeation. *Pharmaceutics* 12:661.
- Kucharz K, Kristensen K, Johnsen KB, et al. (2021). Post-capillary venules are the key locus for transcytosis-mediated brain delivery of therapeutic nanoparticles. *Nat Commun* 12:4121.
- Kumar V, Patiyal S, Kumar R, et al. (2021). B3Pdb: an archive of blood-brain barrier-penetrating peptides. *Brain Struct Funct* 226:2489–95.

- Kumthekar P, Tang S-C, Brenner AJ, et al. (2020). ANG1005, a brain-penetrating peptide–drug conjugate, shows activity in patients with breast cancer with leptomeningeal carcinomatosis and recurrent brain metastases. *Clin Cancer Res* 26:2789–99.
- Lee JH, Engler JA, Collawn JF, Moore BA. (2001). Receptor mediated uptake of peptides that bind the human transferrin receptor. *Eur J Biochem* 268:2004–12.
- Lehtinen J, Magarkar A, Stepniowski M, et al. (2012). Analysis of cause of failure of new targeting peptide in PEGylated liposome: molecular modeling as rational design tool for nanomedicine. *Eur J Pharm Sci* 46:121–30.
- Li Y, Song Y, Zhao L, et al. (2008). Direct labeling and visualization of blood vessels with lipophilic carbocyanine dye Dil. *Nat Protoc* 3:1703–8.
- Libeu CP, Lund-Katz S, Phillips MC, et al. (2001). New Insights into the heparan sulfate proteoglycan-binding activity of apolipoprotein E. *J Biol Chem* 276:39138–44.
- Matsui T, Yoshino A, Tanaka M. (2020). A trip of peptides to the brain. *Food Prod Process and Nutr* 2:30.
- Morito T, Harada R, Iwata R, et al. (2021). Synthesis and pharmacokinetic characterisation of a fluorine-18 labelled brain shuttle peptide fusion dimeric affibody. *Sci Rep* 11:2588.
- Nag O, Awasthi V. (2013). Surface engineering of liposomes for stealth behavior. *Pharmaceutics* 5:542–69.
- Niewoehner J, Bohrmann B, Collin L, et al. (2014). Increased brain penetration and potency of a therapeutic antibody using a monovalent molecular shuttle. *Neuron* 81:49–60.
- Ogawa K, Fuchigami Y, Hagimori M, et al. (2018). Efficient gene transfection to the brain with ultrasound irradiation in mice using stabilized bubble lipopolyplexes prepared by the surface charge regulation method. *IJN* 13:2309–20.
- Ogawa K, Kato N, Kawakami S. (2020). Recent strategies for targeted brain drug delivery. *Chem Pharm Bull (Tokyo)* 68:567–82.
- Oller-Salvia B, Sánchez-Navarro M, Giralte E, Teixidó M. (2016). Blood–brain barrier shuttle peptides: an emerging paradigm for brain delivery. *Chem Soc Rev* 45:4690–707.
- Re F, Cambianica I, Zona C, et al. (2011). Functionalization of liposomes with ApoE-derived peptides at different density affects cellular uptake and drug transport across a blood-brain barrier model. *Nanomedicine* 7:551–9.
- Rousselle C, Clair P, Lefauconnier J-M, et al. (2000). New advances in the transport of doxorubicin through the blood-brain barrier by a peptide vector-mediated strategy. *Mol Pharmacol* 57:679–86.
- Ruan S, Zhou Y, Jiang X, Gao H. (2021). Rethinking CRITID procedure of brain targeting drug delivery: circulation, blood brain barrier recognition, intracellular transport, diseased cell targeting, internalization, and drug release. *Adv Sci (Weinh)* 8:2004025.
- Sauer I, Dunay IR, Weisgraber K, et al. (2005). An apolipoprotein E-derived peptide mediates uptake of sterically stabilized liposomes into brain capillary endothelial cells. *Biochemistry* 44:2021–9.
- Schwarze SR, Ho A, Vocero-Akbani A, Dowdy SF. (1999). In vivo protein transduction: delivery of a biologically active protein into the mouse. *Science* 285:1569–72.
- Suga T, Fuchigami Y, Hagimori M, Kawakami S. (2017). Ligand peptide-grafted PEGylated liposomes using HER2 targeted peptide-lipid derivatives for targeted delivery in breast cancer cells: the effect of serine-glycine repeated peptides as a spacer. *Int J Pharm* 521:361–4.
- Suga T, Kato N, Hagimori M, et al. (2018). Development of high-functionality and -quality lipids with RGD peptide ligands: application for PEGylated liposomes and analysis of intratumoral distribution in a murine colon cancer model [research-article]. *Mol Pharmaceutics* 15:4481–90.
- Urich E, Schmucki R, Ruderisch N, et al. (2015). Cargo delivery into the brain by in vivo identified transport peptides. *Sci Rep* 5:14104.
- Uwamori H, Ono Y, Yamashita T, et al. (2019). Comparison of organ-specific endothelial cells in terms of microvascular formation and endothelial barrier functions. *Microvasc Res* 122:60–70.
- van Rooy I, Mastrobattista E, Storm G, et al. (2011). Comparison of five different targeting ligands to enhance accumulation of liposomes into the brain. *J Control Release* 150:30–6.
- Wang D, El-Amouri SS, Dai M, et al. (2013). Engineering a lysosomal enzyme with a derivative of receptor-binding domain of apoE enables delivery across the blood–brain barrier. *Proc Natl Acad Sci U S A* 110:2999–3004.
- Weksler B, Romero IA, Couraud P-O. (2013). The hCMEC/D3 cell line as a model of the human blood brain barrier. *Fluids Barriers CNS* 10:16.
- Yao H, Wang K, Wang Y, et al. (2015). Enhanced blood–brain barrier penetration and glioma therapy mediated by a new peptide modified gene delivery system. *Biomaterials* 37:345–52.
- Yasaswi PS, Shetty K, Yadav KS. (2021). Temozolomide nano enabled medicine: promises made by the nanocarriers in glioblastoma therapy. *J Control Release* 336:549–71.
- Zhan C, Li B, Hu L, et al. (2011). Micelle-based brain-targeted drug delivery enabled by a nicotine acetylcholine receptor ligand. *Angew Chem Int Ed Engl* 50:5482–5.